Dispersion pre-compensation of 15 femtosecond optical pulses for high-numerical-aperture objectives

M. MÜLLER,* J. SQUIER,† R. WOLLESCHENSKY,‡ U. SIMON§ & G. J. BRAKENHOFF*

*BioCentrum Amsterdam, University of Amsterdam, Institute of Molecular Cell Biology, Kruislaan 316, 1098 SM Amsterdam, The Netherlands

†Department of Electrical and Computer Engineering, University of California, San Diego, 9500 Gilman Drive, La Jolla, CA 92093, U.S.A.

‡Carl Zeiss Jena GmbH, Zeiss Group, D-07740 Jena, Germany

§Friedrich Schiller University Jena, Institute of Optics and Quantumelectronics, Max-Wien-Platz 1, 07743 Jena, Germany

Summary

The excitation efficiency in two-photon absorption (TPA) microscopy depends strongly – owing to the square dependence of the TPA fluorescence on the excitation intensity – on the temporal width of the excitation pulse. Because of their inherently large frequency bandwidth, ultrashort optical pulses tend to broaden substantially because of dispersion from propagation through the dispersive elements in the microscope. In this paper, the dispersion characteristics of a wide range of microscope objectives are investigated. It is shown that the induced dispersion can be pre-compensated in all cases for pulses as short as 15 fs. Because of the excellent agreement between the results from theoretical modelling and the experimental data, predictions of the possibility of dispersion control for microscope objectives in general, as well as for even shorter pulses, can be inferred. Since for TPA imaging the background due to single photon absorption processes and scattering is independent of the pulse width, proper dispersion pre-compensation – which minimizes the pulse duration at the focal point and hence maximizes the excitation efficiency – provides optimal image contrast in TPA microscopy.

Introduction

Two-photon absorption (TPA) microscopy (Denk *et al.*, 1990; Webb, 1990; Piston & Webb, 1991) incorporates a number of features that make it attractive for specific areas of biological research. Owing to the non-linear nature of the excitation process – the absorption probability depends quadratically on the excitation intensity, the excitation of fluorophores in a specimen is typically limited to the small three-dimensional volume as defined by the focusing properties of the microscope objective. This results both in automatic sectioning – with a resolution slightly inferior to its single-photon analogue (Sheppard & Gu, 1990; Sheppard & Gu, 1992; Deitche *et al.*, 1994; Gu & Sheppard, 1995; Gu *et al.*, 1995; Kano *et al.*, 1996) – and in reduced out-of-focus photobleaching. Additionally, an increased penetration in scattering samples results from the longer excitation wavelength (typically in the near-infrared) used.

The combination of these features has attracted considerable interest from the biological community and has already resulted in a fair number of publications, demonstrating the feasibility of the technique in practice (e.g. Piston & Webb, 1991; Denk *et al.*, 1994; Piston *et al.*, 1994; Piston *et al.*, 1995; Brakenhoff *et al.*, 1996b; Svoboda *et al.*, 1996; Yu *et al.*, 1996). Although much of the TPA process in fluorophores is not yet understood in detail, it appears that many commonly used fluorescing stains have sufficiently large TPA absorption cross-sections for practical TPA microscopy purposes. More detailed research in this area (Xu & Webb, 1996; Xu *et al.*, 1996) will improve our insight and possibly lead to specific TPA stains. There is relatively little information available with respect to the induced radiation damage at the biological level by TPA microscopy and how it compares to its single-photon analogue (Brakenhoff *et al.*, 1996a; König *et al.*, 1996; König *et al.*, 1997).

Owing to the inherently large frequency bandwidth of

Correspondence to: M. Müller. Tel.: 31 205 256 211; fax: 31 205 256 221; email: muller@mc.bio.uva.nl

the ultrashort optical pulses used in TPA microscopy (typically < 150 fs), propagation of these pulses through an optical system such as a microscope induces substantial dispersion. A large part of the induced dispersion is due to the microscope objective which consists of a large number of (highly) dispersive elements. Any relay elements within the microscope will introduce additional dispersion. If left uncompensated, dispersion causes the optical pulses to broaden in time, reducing the TPA efficiency. Typically the TPA efficiency drops slightly stronger than linearly with increasing pulse width, owing to changes in the shape of the dispersed pulse. Knowledge of the dispersion characteristics of high-numerical aperture (NA) microscope objectives permits the use of pre-compensation techniques to retain temporal pulse integrity at the focal point of the objective. In this paper, the influence of dispersion in microscopy with ultrashort optical pulses and the possibilities for dispersion pre-compensation in microscopical systems is treated in a general and fundamental manner. Although demonstrated

in the context of TPA microscopy, the results presented provide an understanding of the way to create the proper focusing conditions for ultrashort optical pulses. This is of special interest, not only for TPA microscopy, but also for other areas of research, such as multiphoton absorption imaging (e.g. Hell *et al.*, 1996; Szmacinski *et al.*, 1996), fluorescence lifetime imaging (Müller *et al.*, 1995a; Buist *et al.*, 1996) and optical coherence tomography (e.g. Fujimoto *et al.*, 1986; Huang *et al.*, 1991).

A number of groups have addressed this issue of dispersion of ultrashort pulses in microscope objectives (Hänninen & Hell, 1994; Brakenhoff *et al.*, 1995; Müller *et al.*, 1995b; Guild *et al.*, 1997). In this paper we present the results of dispersion measurements of 15 fs pulses through a number of different high-NA microscope objectives. At 800 nm a transform limited, Sech^2 shaped, 15 fs pulse corresponds to a bandwidth of ≈ 45 nm ($\Delta v \Delta \tau = 0.315$). This large bandwidth implies that higher order (cubic and quartic) dispersion terms become non-negligible both for the dispersion induced by the objective and for the pre-compensation technique used to cancel it. Hence, these ultrashort pulses provide a stringent test for the dispersion pre-compensation technique, the measurement technique of the actual pulse width as well as for the theoretical model developed to describe the observed dispersion.

Using dispersive ray-tracing calculations to model the dispersion induced by a typical objective and comparing the results with the experimental data, general predictions with respect to dispersion control in microscope objectives can be inferred. The experiments confirm the validity of our theoretical model, which in turn permits detailed design of the optimal configurations for TPA microscopy or time-resolved microscopy with ultrashort optical pulses.
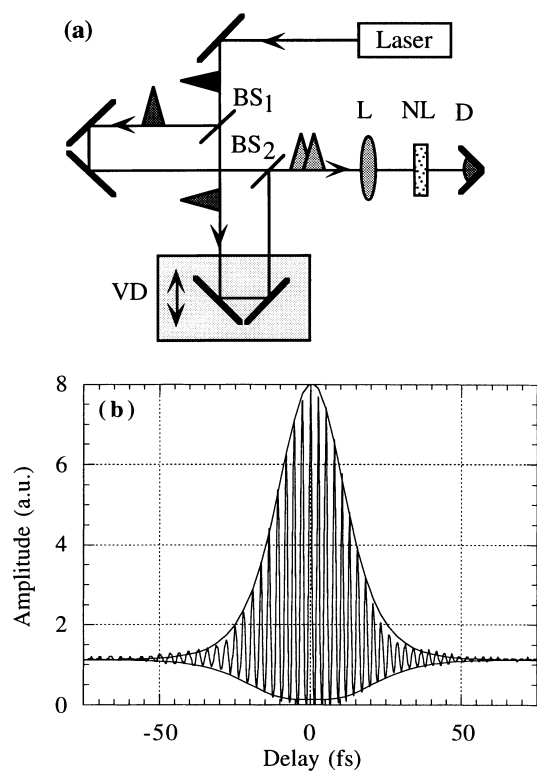
2. Measurement and control of femtosecond pulses

2.1. Two-photon absorption autocorrelation

To examine the effects of dispersion on the ultrashort optical pulses used in TPA microscopy and to enable proper pre-compensation, it is important to be able to measure the pulse width at the focal point of a high-NA microscope objective. To this end, we developed the two-photon absorption autocorrelation (TPAA) technique (Brakenhoff *et al.*, 1995; Müller *et al.*, 1995b), which we will briefly describe here.

A general autocorrelation set-up is schematically depicted in Fig. 1(a). The input laser beam is split into two parts by a 50% beamsplitter. One of the beams passes a variable delay line before it is recombined with the other beam by a second 50% beamsplitter. Two beamsplitters – with their coated side orientated in opposite directions – are used instead of one, to ensure that both beams experience the same dispersion in the – so-called balanced

Fig. 1. (a) Schematic of a general balanced autocorrelation set-up. BS: beamsplitter; VD: variable delay; L: lens; NL: non-linear medium; D: detector. (b) SHG interferometric autocorrelation trace of the laser pulses used in the experiments. Fitting the data, assuming Sech^2 shaped input pulses, yields a pulse width of 15·5 fs. Given the measured spectral bandwidth of 2.4×10^{13} Hz, this corresponds to an almost transform limited pulse with a time-bandwidth product of $\Delta v \Delta t \sim 0.37$.

– autocorrelator. The two co-propagating beams are focused into a medium, the non-linear response of which is detected as a function of the relative delay between the two beams. This delay is varied by changing the optical path length in one of the arms of the autocorrelator. Note that the response needs to be non-linear to allow measurement of the autocorrelation of the pulse envelope rather than of the coherence time of the pulse (Diels & Rudolph, 1996). Since the beams co-propagate, the signal will show interference fringes as a function of delay, which are used as an internal time calibration in the measurement. This is especially important to permit accurate measurement of ultrashort optical pulses. A typical interferometric second harmonic generation (SHG) autocorrelation trace is shown in Fig. 1(b), showing the 1:8 ratio of baseline and maximum with respect to the background. The best fit to the data was obtained for a $Sech^2$ input pulse of $15 \cdot 5$ fs. The flatness of the baseline indicates a transform limited input pulse, which is confirmed by the measured time-bandwidth product of $\Delta v \Delta t \approx 0 \cdot 37$.

In conventional pulse measurements, the non-linear medium is a crystal in which a second harmonic signal is generated. The SHG process dictates stringent phase-matching conditions, which limit the signal generation to a small ($\leq 10°$) acceptance angle of the input radiation with respect to the orientation of the crystal. Since high-NA objectives focus radiation over angles up to $120°$ the SHG process is not suitable for pulse width measurement in this case. In the TPAA technique detection of the fluorescence generated in a TPA process is used as the non-linear response. Since an isotropic fluorescing medium can be used in this case, the TPA process is not limited by phase-matching and has the additional advantage that it can be used in a medium which closely resembles microscopy practice.

2.2. Dispersion pre-compensation

To understand the nature of the dispersive effects of different media or optical devices on ultrashort pulses it is most convenient to express the frequency dependent phase $\phi(\omega)$ of
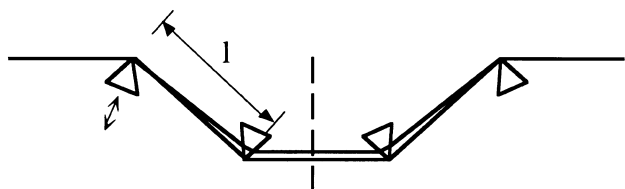

Fig. 2. General schematic of double prism pair dispersion pre-compensation unit. The tip-to-tip prism spacing (l), and the amount that each tip is inserted into the beam determines the net amount of dispersion, as well as the sign.

the ultrashort pulse in terms of a Taylor series as in Eq. (1).

$$\varphi(\omega) = \varphi(\omega_0) + \left(\frac{d\varphi}{d\omega}\right)_{w_0} (\omega - \omega_0)$$
$$+ \frac{1}{2!}\left(\frac{d^2\varphi}{d\omega^2}\right)_{w_0}(\omega - \omega_0)^2 \ldots \tag{1}$$

where ω_0 denotes the centre frequency of the pulse. Given the known functional dependence of the refractive index with respect to wavelength, $n(\lambda)$, it is usually convenient to express the different terms in the expansion of Eq. (1) in terms of the derivative of the refractive index with respect to the wavelength:

$$\varphi_1 = \frac{L}{c}\left[n(\lambda_0) - \lambda_0\left(\frac{dn}{d\lambda}\right)_{\lambda_0}\right] \tag{2a}$$

$$\varphi_2 = \frac{1}{2!}\frac{L}{c}\cdot\left(\frac{\lambda_0}{2\pi c}\right)\cdot\left[\lambda_0^2\left(\frac{d^2n}{d\lambda^2}\right)_{\lambda_0}\right] \tag{2b}$$

$$\varphi_3 = \frac{1}{3!}\frac{L}{c}\cdot\left(\frac{\lambda_0}{2\pi c}\right)^2\cdot\left[3\lambda_0^2\left(\frac{d^2n}{d\lambda^2}\right)_{\lambda_0} + \lambda_0^3\left(\frac{d^3n}{d\lambda^3}\right)_{\lambda_0}\right] \tag{2c}$$

$$\varphi_4 = \frac{1}{4!}\frac{L}{c}\cdot\left(\frac{\lambda_0}{2\pi c}\right)^3$$
$$\times\left[12\lambda_0^2\left(\frac{d^2n}{d\lambda^2}\right)_{\lambda_0} + 8\lambda_0^3\left(\frac{d^3n}{d\lambda^3}\right)_{\lambda_0} + \lambda_0^4\left(\frac{d^4n}{d^4}\right)\right] \tag{2d}$$

where L is the pathlength through the dispersive material and c is the speed of light. The first derivative in this series (ϕ_1) represents the group delay (GD) of the wave packet and is indicative of the time-of-flight through the optical system. The second order term (ϕ_2), is the group delay dispersion (GDD). A non-zero value for the GDD indicates that the pulse width is increased from its transform limit. While the GDD broadens the pulse width, the existence of a third order dispersion (TOD; ϕ_3) results in an asymmetric pulse distortion. Fourth order dispersion (FOD; ϕ_4) once again, relates to a pulse broadening. The degree to which each of these terms affects the pulse width and shape is dependent on the pulse bandwidth and the length of the optical path that the pulse propagates through the dispersive material. For the pulse widths and material path lengths considered here it is important to know the amount and sign of the dispersion through fourth order for each element in the optical system.

In the near IR (800 nm), the GDD, TOD and FOD are all positive for most common glasses (however, this should never be assumed, the sign and amount of dispersion for a material in the system should always be carefully determined). Thus, to compensate for a net positive residual phase error, a dispersive system capable of producing negative GDD, TOD and FOD must be used. Changing the sign of the dispersion can be done readily using a prism pair (Fork *et al.*, 1984), or grating pair (Treacy, 1969). The negative dispersion arises from the angular dispersion

produced by these devices. For the amounts and signs of dispersion considered here, the prism pair is the most adequate match for compensation, capable of producing negative GDD, TOD and FOD. In contrast, the standard grating pair produces negative GDD, but positive TOD, which results in a cancellation of the GDD term, but a net increase in the TOD.

The basic prism dispersion compensation scheme is illustrated in Fig. 2. The first prism creates an angular dispersed beam, and the second prism is used to limit this angular dispersion, recollimating the beam into a specularly dispersed, yet parallel output (it is spatially chirped). The tip-to-tip prism spacing (l), and the amount that each tip is inserted into the beam determines the net amount of dispersion, as well as the sign. In order to remove the spatial chirp the prism system must be double passed, which also doubles the amount of dispersion obtained for a given prism spacing.

Unfortunately, for most systems the rate at which the GDD to TOD dispersion increases is very different between the prism pair and the material path length one is attempting to compensate for. This means that while the prism pair can effectively cancel out the material GDD, there is a residual TOD resulting from the prism pair. This residual TOD can limit the final achievable pulse width. The amount of residual TOD can be controlled by several methods, a few of which are described here. Most important is the choice of prism material. Highly dispersive glasses such as SF10 leave a larger residual TOD, and can easily limit the compressed pulse width. For the pulse durations considered here, fused silica prisms are a much better match, helping to minimize the residual TOD, and making it possible to achieve much shorter pulse durations.

Another method of helping to achieve TOD compensation arises from the use of dielectric mirror coatings. For the mirrors used here in the roof mirror assembly of the prism compensator (CVI TLM1, s-polarization, 45° angle of incidence) $\approx 12\,\mathrm{fs}^3$ of correction is acquired per reflection. (Note: all other mirrors were protected silver, adding negligible dispersion.) Multiple reflections from mirrors with this coating (or other dielectric coatings providing even higher dispersion for that matter) could be used to increase this number to help further balance out the residual TOD due to the prism sequence.

3. Focusing 15 fs optical pulses

To obtain a general understanding of the dispersion characteristics of microscope objectives, six different high-NA microscope objectives were measured. The objectives are listed in Table 1 with their shorthand notation used in the rest of this paper. All objectives are corrected for infinity.

3.1. Experimental set-up

The experimental set-up for measuring the TPAA signal is depicted in Fig. 3. The laser is a home-built Ti : sapphire oscillator operating at 800 nm, 76 MHz, with an average power of $\approx 150\,\mathrm{mW}$. The pulse width – measured with SHG autocorrelation (see Fig. 1b) – is 15·5 fs. The beam first passes a dispersion pre-compensation unit (Fig. 3b, see details below) before being split and recombined in a
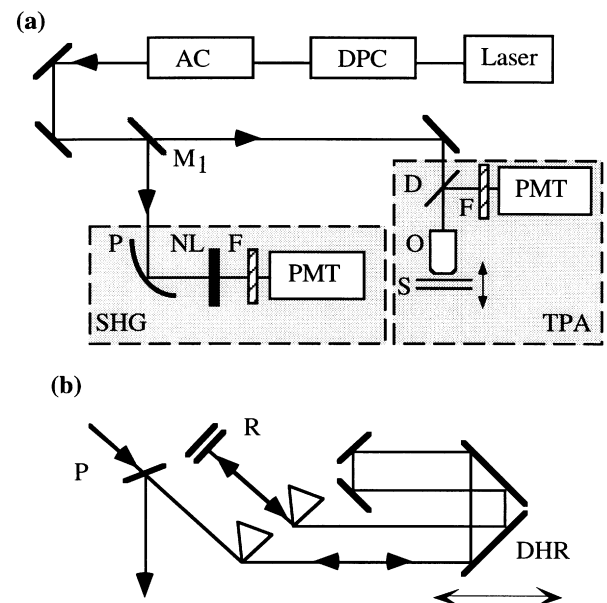

Fig. 3. (a) Schematic of the experimental set-up. DPC: dispersion pre-compensation unit; AC: balanced autocorrelation unit as depicted in Fig. 1(a); M_1: insertable mirror; P: parabolic focusing mirror; NL: 100 μm, type I KDP doubling crystal; F: BG39 blocking filter; PMT: photomultiplier tube; D: dichroic mirror; O: microscope objective; S: sample on an axial translation stage. (b) Doubly folded double prism pair dispersion pre-compensation unit. DHR: dihedral reflector; R: roof mirror assembly; P: pick-off mirror. The roof mirror reflects the beam back in a plane parallel to, but above, the plane of incidence. The dihedral reflector is mounted on a translation rail allowing the optical path length between the two prisms to be varied.

Table 1. Microscope objectives for dispersion measurements.

Objective	Shorthand
Zeiss C-Apochromat 63×/1·2 W Korr	A
Zeiss C-Apochromat 40×/1·2 W Korr	B
Zeiss Plan Neofluar 100×/1·3 oil	C
Zeiss Plan Neofluar 63×/1·25 oil	D
Zeiss Plan Neofluar 40×/1·3 oil	E
Zeiss CP-Achromat 100×/1·3 oil	F

balanced autocorrelation unit. The output of this unit can be directed to generate either a SHG autocorrelation trace, or a TPAA signal. Owing to losses on the mirrors – mainly on the gold-coated dihedral reflector DHR, only $\approx 35\,mW$ remains to go into the TPAA part of the set-up. The SHG, as well as the TPAA, signal is detected by a photomultiplier tube and digitized by a digital oscilloscope (Le Croy 9361). A BG39 blocking filter blocks out any scattered light at the laser wavelength.

There are a number of points to note about this set-up. Putting in or taking out mirror M_1 quickly changes the set-up from conventional interferometric SHG autocorrelation to TPAA, providing the opportunity to determine the absolute pulse broadening induced by the objective, relative to the shortest pulse obtainable for the system. A parabolic focusing mirror and a $100\,\mu m$, type I KDP doubling crystal render the SHG autocorrelator practically dispersion free.

The dispersion pre-compensation unit consists of a doubly folded double prism pair arrangement (Fig. 3b). The prisms are of fused silica, which has a low angular dispersion. This minimizes the residual TOD induced by the prisms (see above). Owing to this low dispersion the prisms have to be separated over a relatively long distance to induce substantial dispersion compensation. Because of the angular spread of the beam between the prisms, the physical size of the prisms ultimately limits the maximum separation distance between them. At larger distances the spectrum is clipped, which would cause a broadening of the pulse. Measurement of the spectrum of the pulses after the dispersion pre-compensation unit confirmed that no clipping of the spectrum affected the TPAA measurements reported here for all prism separation settings.

In the TPAA experiments the sample consisted of a $10^{-3}\,M$ solution of Rhodamine 6G in water, contained in a 0·1 mm microslide (Vitro Dynamics, Rockaway, NJ). The fluorescence is measured in the backscattering direction. The dispersion induced by the dichroic mirror was measured to be negligible. The objectives are used without additional tube lens. The beam diameter was $\approx 5\,mm$ (FWHM), in most cases substantially underfilling the objective's pupil diameter, which ranges from 4·3 to 10·7 mm for the objectives used.

In all measurements the TPAA responses were analysed by fitting the signal to the theoretical autocorrelation trace (Diels & Rudolph, 1996). In almost all cases the best fit was obtained by assuming $Sech^2$, rather than Gaussian, shaped input pulses. For consistency we report the pulse width and amplitude obtained for a $Sech^2$ fit throughout the rest of this paper. It should be noted that this fitting procedure gives an exactly correct result for the pulse width only if the pulses
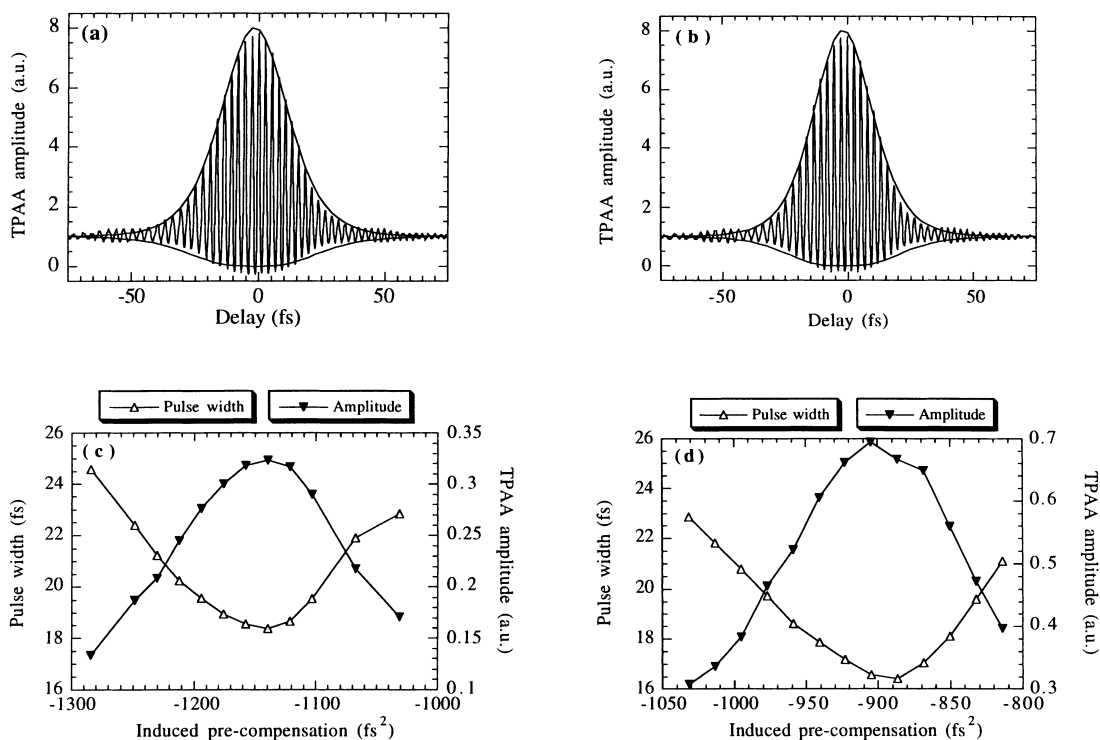

Fig. 4. (a) and (b) TPAA autocorrelation traces for objectives A and D, respectively, at the dispersion pre-compensation setting that produces the minimum pulse width at focus. (c) and (d) TPAA pulse width and amplitude for objectives A and D, respectively, as a function of induced dispersion pre-compensation.

Table 2. Dispersion pre-compensation values for microscope objectives.

Objective	A	B	C	D	E	F	SHG
Pulse width (fs)	18·4	18·4	14·7	16·4	17·5	15·9	15·5
GDD (fs^2)	−1140	−1104	−778	−887	−1104	−579	0

are transform limited and are indeed Sech^2 shaped. Deviations from either of these conditions, together with slight misalignment of the autocorrelator, will introduce a (systematic) error in the calculated pulse width. Hence, although the error in the measured pulse width resulting from noise is very low ($\approx 1\%$), we estimate the absolute accuracy of the pulse width measurement in the manner described above at approximately ($\pm 5\%$).

4. TPAA measurements for the Zeiss objectives

For all objectives the pulse width at the focal point was measured as a function of induced dispersion pre-compensation using TPAA. Typical results of such measurements for the objectives A and D are shown in Fig. 4. Two important points should be noted from these figures. First, despite the large amount of dispersion induced by the objectives – no TPAA signal could be observed prior to pre-compensation – proper dispersion pre-compensation restores the original pulse width at the focal point of the high-NA microscope objective. Second, the TPA efficiency is a function of the pulse width, generating the maximum signal at the minimum pulse width. The dependence of the

TPAA signal on the pulse width is stronger than linear, which can be understood from a reshaping of the pulse from more Gaussian for non-transform limited pulses to almost Sech^2 at the minimum pulse width. Table 2 and Fig. 5 summarize the results, with the minimum pulse width, measured with the TPAA technique, for all objectives and the amount of GDD, induced by the dispersion pre-compensation unit, required to obtain this minimum.

Note that the pulse width shows a slight increase with increasing GDD to be compensated. This is due to the fact that for larger pre-compensation values the residual TOD from the dispersion pre-compensation unit introduces increasing amounts of broadening. Hence this is not due to the objectives, but rather is related to the particular pre-compensation configuration used. Note also that, as expected, increasing amounts of dispersion need to be pre-compensated by for objectives containing a larger number of dispersive elements. In all cases, however, the induced dispersion is primarily second order and can thus be pre-compensated in a straightforward manner. It should be kept in mind that Table 2 refers to the dispersion induced by the objective only. In a complete microscope the induced dispersion can be substantially larger (> 5 times,
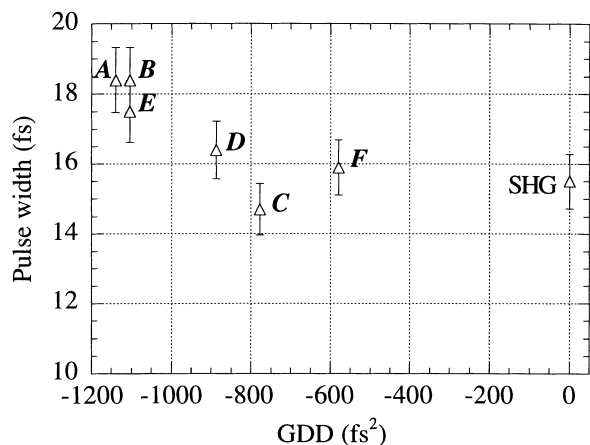

Fig. 5. Minimum autocorrelation pulse width measured for SHG and TPAA with the microscope objectives as a function of induced dispersion pre-compensation. The increase in pulse width with larger pre-compensation is due to the residual TOD produced by the dispersion pre-compensation unit.
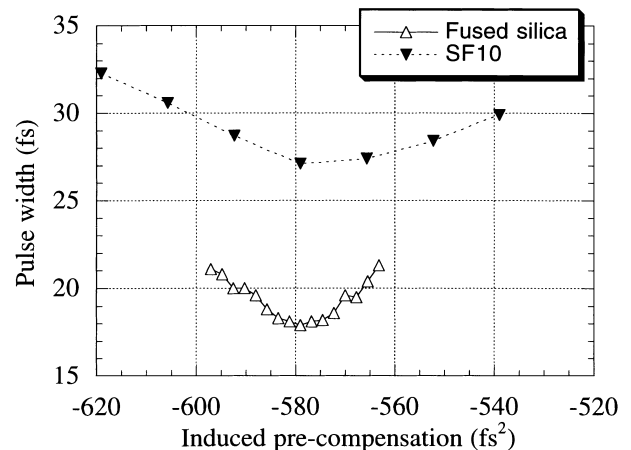

Fig. 6. TPAA pulse width for objective *F* as a function of induced dispersion pre-compensation, for fused silica and SF10 prisms. Residual TOD from the prism material in the dispersion pre-compensation unit limits the minimum pulse width that can be obtained.

see Section 5) when a beam expander and scan lens have to be included.

To demonstrate the effect of residual TOD produced by a dispersion pre-compensation unit, we repeated the measurements after replacing the fused silica prisms by SF10 prisms. SF10 has a much larger angular dispersion than fused silica. Hence it is to be expected that in cases where large amounts of dispersion have to be pre-compensated, the residual TOD becomes the limiting factor. This is demonstrated in Fig. 6 where the TPAA pulse width is plotted as a function of induced dispersion pre-compensation for both the set-up with fused silica prisms and the one with SF10 prisms. Note that these measurements were done with a slightly differently aligned Ti : sapphire oscillator running at 17·5 fs. Clearly the SF10 dispersion pre-compensation set-up cannot restore the original pulse width due to residual TOD. A similar effect was observed by (Guild *et al.*, 1997).

Numerically the matching of the dispersion characteristics of the prism material with respect to those of the microscope objective to be compensated for can be exemplified as follows. With dispersive ray-tracing (see below) the relative rates of TOD to GDD effectively induced by objective F are calculated to be $(\phi_3/\phi_2)_F \approx 0\cdot23$ fs. A similar calculation for the prism pair dispersion pre-compensation unit yields $(\phi_3/\phi_2)^{\text{prism}}_{\text{fused silica}} \approx 0\cdot36$ fs and $(\phi_3/\phi_2)^{\text{prism}}_{\text{SF10}} \approx 1\cdot32$ fs for the fused silica and SF10 prisms, respectively. Clearly the former provide a better match to the dispersion induced by the objective.

4.1. Theoretical modelling

In dispersive ray-tracing, the contribution of all dispersion terms of Eq. (2) is calculated along each ray through the optical system. The total dispersion is the sum of the dispersion induced by each of the dispersive elements in the system. Since this calculation is based on ray-tracing, any additional effects caused by the interplay of beam diffraction and angular dispersion are neglected.

Based on known optical data, a dispersive ray-tracing calculation was performed for objective *F*. For the on-axis ray through the objective, at a carrier wavelength $\lambda_0 = 800$ nm, the various orders of dispersion were calculated to be: GDD = 579·4 fs^2; TOD = 129·9 fs^3 and FOD = 24·3 fs^4. Based on the same principles of dispersive ray-tracing, the induced dispersion at each setting of the dispersion pre-compensation unit (Fig. 3b) can be calculated. The setting for the minimum TPAA pulse width for objective F – which in this experimental set-up corresponds to a (single pass) prism separation of 877 mm – is calculated to correspond to GDD = − 579 fs^2; TOD = − 209 fs^3 and FOD = − 156 fs^4. This includes the dispersion of the coatings in the dispersion pre-compensation unit. When the net dispersion of the system is used (dispersion pre-compensation unit plus objective dispersion) it is

calculated that a 15·5 fs Sech^2 pulse should only broaden by ∼0·8 fs, which is in excellent agreement with the measured pulse broadening. The agreement between experiment and dispersive ray-tracing calculations shows that diffraction and angular dispersion are negligible in this case.

To provide a general feeling of the dispersion induced by objective F (GDD = 597·4 fs^2; TOD = 129·9 fs^3 and FOD = 24·3 fs^4) – which may serve as a low end estimate for the typical amount of dispersion induced by an objective in TPA microscopy – the broadening of a 15 and 40 fs pulse was calculated with dispersive ray-tracing. Under these conditions it is found that, if uncompensated, a transform-limited 15 fs pulse broadens to 210 fs, whereas a transform-limited 40 fs pulse broadens to only 87 fs. This clearly shows the effect of frequency bandwidth on the broadening induced for a given amount dispersion.

4.2 General remarks

The fact that the minimum TPAA pulse width equals the pulse width obtained with SHG autocorrelation – including the residual TOD from the dispersion pre-compensation unit – demonstrates that there is negligible sample induced broadening. This was further substantiated in independent experiments, where the KDP crystal was substituted for a solution of rhodamine 6G, and the all reflective optic geometry was used.

In the experiments reported in this section, the aperture of the objective was underfilled on purpose to reduce the sensitivity of the measurement to pulse-broadening induced by a radially varying GD, also known as phase time delay (PTD) (Bor, 1988; Bor, 1992) or radially varying higher order dispersion terms. In a separate series of measurements we investigated this issue in detail (Müller *et al.*, in preparation).

Finally, it should be noted generally that the 8:1 contrast in an interferometric TPAA trace decreases owing to radially varying group delay or higher order dispersion terms, and/ or high-NA focusing conditions.

5. Dispersion pre-compensation and TPA imaging

To demonstrate visually the effect of dispersion pre-compensation in TPA microscopy, the general principle, as described above, was applied to a practical TPA imaging set-up. The set-up consisted of a Coherent MIRA 900F Ti:Sapphire laser, running at 800 nm, 80 MHz. The laser output was sent through a SF10 prism pair dispersion pre-compensation unit and coupled into a Zeiss confocal laser scanning microscope, LSM 410 invert, and focused down with objective *E*. The pulse width of the laser, measured with SHG autocorrelation, was 127 ± 10 fs. Using the TPAA technique, it was found that the complete microscope set-up
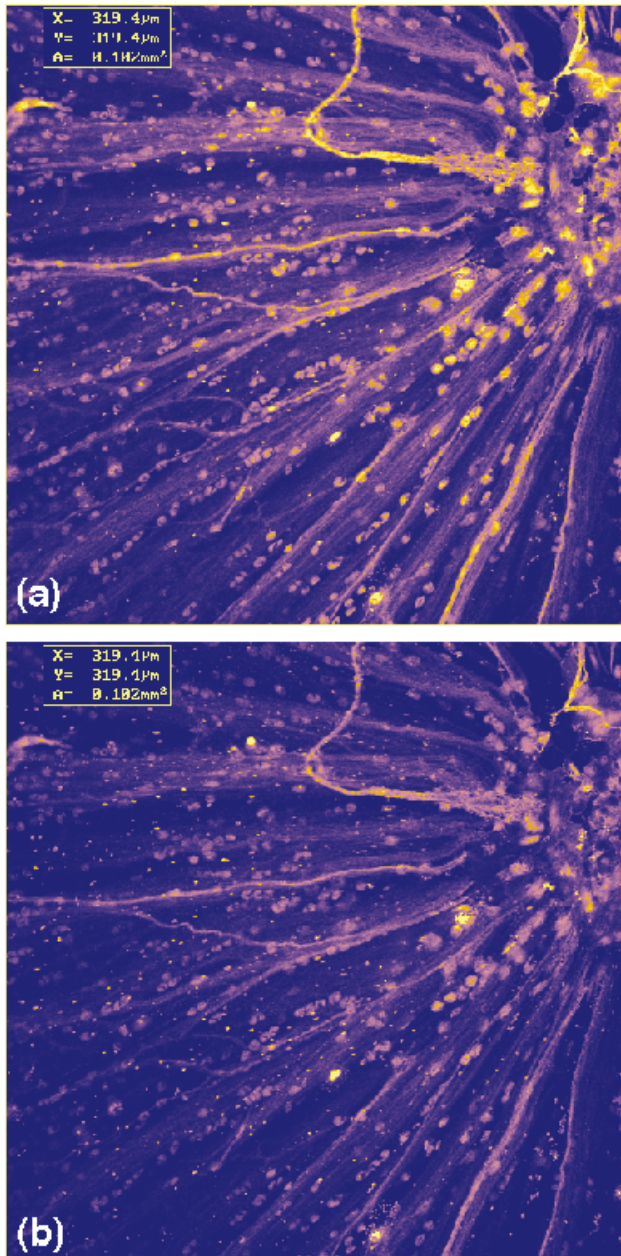
Fig. 7. TPA images of the retina of a fish eye, using a DAPI stain dissolved in the nucleus of the retina cells and a FITC/rhodamine stain attached to the nerve cell fibres: (a) 170 fs pulse at a setting of the dispersion pre-compensation unit for minimum pulse width at the focal point; (b) 340 fs pulse obtained by translating one of the prisms in the dispersion pre-compensation unit with respect to (a). All other experimental conditions are identical and both images are plotted on the same false colour scale.

broadened the pulse to 218 ± 10 fs. This indicates an induced dispersion of $\approx 4500 \pm 600$ fs^2 (for a Gaussian input pulse), which is consistent with the dispersion calculated from the optical data of 5120 fs^2 for an on-axis beam travelling through the whole microscope, including

the objective lens and the external beam expander. Objective *E* alone induces a GDD of 1100 fs^2 (see Table 2), indicating that the total dispersion is dominated by the relay lenses and other optical components such as filters and dichroics inside the microscope. A minimum pulse width of 170 ± 10 fs at the focal point of the microscope was obtained by optimizing the dispersion pre-compensation unit.

Figure 7 shows the increase ($> 70\%$) in TPA fluorescence intensity when the input pulse width is decreased by adjusting the dispersion pre-compensation unit. Note, that since the scattering- and single-photon-induced background is independent of the input pulse width, this TPA intensity increase results in an improved image contrast. Figure 7(a) shows a TPA image of the retina of a fish eye with double staining: DAPI dissolved in the nucleus of retina cells; and FITC/rhodamine attached to the nerve cell fibres. The average input power is 2 mW. The dispersion pre-compensation unit is set for the minimum pulse width of 170 fs at the focal point. Figure 7(b) shows another image of the same specimen, where the pulse width has been increased to 340 fs by translating one of the prisms in the prism pair dispersion pre-compensation unit. All other experimental conditions are identical and the images are plotted on the same false colour scale. A similar increase in fluorescence intensity could have been obtained by raising the input power by $> 30\%$. The important point is that the fluorescence intensity can be optimized for a given average power merely by choosing the proper dispersion pre-compensation conditions, thereby maximizing the detection efficiency for a given radiation load on the sample.

6. Discussion

We have shown that with proper predispersion compensation it is possible to focus optical pulses as short as 15 fs pulses with a range of high-NA microscope objectives. Since at constant pulse power the TPA probability increases at least linearly with decreasing pulse width, the generated fluorescence from TPA is increased by almost an order of magnitude in reducing the pulse width from the 100 fs level typically used in TPA microscopy today to the 15 fs level. Note that this increase in fluorescence intensity is attained at equal average input power.

By using ultrashort 15 fs optical pulses, which have an inherently large frequency bandwidth and are thus very dispersion sensitive, the measurement technique (TPAA), the dispersion pre-compensation method and the theoretical modelling of the system by dispersive ray-tracing have been tested thoroughly. We obtained excellent agreement between theory and experiment. This agreement makes us confident that it is possible to choose the proper dispersion pre-compensation configuration for any microscope objective, or microscopic system, to retain optical pulse integrity

at the focal point. Furthermore, with proper accounting of higher order dispersion, and a properly designed pre-compensator, there appears to be no fundamental reason why even shorter pulses cannot be properly focused by these objectives. With the theoretical understanding of the dispersion properties of high-NA lenses an optimal dispersion pre-compensation unit can be designed for any practical (microscope) configuration.

Mirror coatings, which are not specially designed for ultrashort pulses, can introduce substantial dispersion. Inside a microscope, such mirrors may induce dispersion (primarily third order) which in principle can be used to reduce the residual TOD due to the prism pre-compensator unit. Alternatively, unaccounted mirror dispersion can also broaden the pulse. Such pulse distortion in turn reduces the TPA efficiency. The TPAA technique provides a tool to measure the actual pulse width at the focal point, including the dispersion induced by the whole system.

The findings of this paper are relevant not only to TPA microscopy but to all optical techniques which rely on strong focusing of ultrashort pulses, such as spatially resolved non-linear optics or time-resolved imaging.

Acknowledgments

References

Bor, Z. (1988) Distortion of femtosecond laser pulses in lenses and lens systems. *J. Mod. Opt.* **35**, 1907–18.

Bor, Z. (1992) Distortion of femtosecond laser pulses in lenses. Wave optical description. *Opt. Commun.* **94**, 249–258.

Brakenhoff, G.J., Müller, M. & Squier, J. (1995) Femtosecond pulse width control. in microscopy by Two-photon absorption auto-correlation. *J. Microsc.* **179**, 253–260.

Brakenhoff, G.J., Müller, M. & Ghauharali, R.I. (1996a) Analysis of efficiency of two-photon versus single-photon absorption for fluorescence generation in biological objects. *J. Microsc.* **183**, 140–144.

Brakenhoff, G.J., Squier, J., Norris, T., Bliton, A.C., Wade, M.H. & Athey, B. (1996b) Real-time two-photon confocal microscopy using a femtosecond, amplified Ti:sapphire system. *J. Microsc.* **181**, 253–259.

Buist, A.H., Müller, M., Gijsbers, E.J., Brakenhoff, G.J., Sosnowski, T.S., Norris, T.B. & Squier, J. (1996) Double pulse fluorescence lifetime measurements. *J. Microsc.* **186**, 212–220.

Deitche, J., Kempe, M. & Rudolph, W. (1994) Resolution in nonlinear laser scanning microscopy. *J. Microsc.* **174**, 69–73.

Denk, W., Delaney, K.R., Gelperin, A., Kleinfeld, D., Strowbridge, B.W., Tank, D.W. & Yuste, R. (1994) Anatomical and functional imaging of neurons using 2-photon laser scanning microscopy. *J. Neuroscience Meth.* **54**, 151–162.

Denk, W., Strickler, J.H. & Webb, W.W. (1990) Two-photon laser scanning fluorescence microscopy. *Science*, **248**, 73–76.

Diels, J.-C. & Rudolph, W. (1996) *Ultrashort Laser Pulse Phenomena. Optics and Photonics* (ed. by P. F. Liao, P. L. Kelley, and I. Kaminow). Academic Press, San Diego, CA.

Fork, R.L., Martinez, O.E. & Gordon, J.P. (1984) Negative dispersion using pairs of prisms. *Opt. Lett.* **9**, 150–152.

Fujimoto, J.G., Silvestri, S.D., Ippen, E.P., Puliafito, C.a., Margolis, R. & Oseroff, a. (1986) Femtosecond optical ranging in biological systems. *Opt. Lett.* **11**, 150–152.

Gu, M. & Sheppard, J.R. (1995) Comparison of three-dimensional imaging properties between two-photon and single-photon fluorescence microscopy. *J. Microsc.* **177**, 128–137.

Gu, M., Tannous, T. & Sheppard, C.J.R. (1995) Three-dimensional confocal fluorescence imaging under ultrashort pulse illumination. *Opt. Commun.* **117**, 406–412.

Guild, J.B., Xu, C. & Webb, W.W. (1997) Measurement of group delay dispersion of high numerical aperture lenses using two-photon excited fluorescence. *Appl. Opt.* **36**, 397–401.

Hänninen, P.E. & Hell, S.W. (1994) Femtosecond pulse broadening in the focal region of a two-photon fluorescence microscope. *Bioimaging*, **2**, 117–121.

Hell, S.W., Bahlmann, K., Schrader, M., Soini, a., Malak, H., Gryczynski, I. & Lakowicz, J.R. (1996) Three-photon excitation in fluorescence microscopy. *J. Biomed. Opt.* **1**, 71–74.

Huang, D., Swanson, E.a., Lin, C.P., Schuman, J.S., Stinson, W.G., Chang, W., Hee, M.R., Flotte, T., Gregory, K., Puliafito, C.a. & Fujimoto, J.G. (1991) Optical coherence tomography. *Science*, **254**, 1178–1181.

Kano, H., van der Voort, H.T.M., Schrader, M., van Kempen, G.M.P. & Hell, S.W. (1996) Avalanche photodiode detection with object scanning and image restoration provides 2–4 fold resolution increase in two-photon fluorescence microscopy. *Bioimaging*, **4**, 187–197.

König, K., So, P.T.C., Mantulin, W.W. & Gratton, E. (1997) Cellular response to near-infrared femtosecond laser pulses in two-photon microscopy. *Opt. Lett.* **22**, 135–137.

König, K., So, P.T.C., Mantulin, W.W., Tromberg, B.J. & Gratton, E. (1996) Two-photon excited lifetime imaging of autofluorescence in cells during UVA and NIR photostress. *J. Microsc.* **183**, 197–204.

Müller, M., Ghauharali, R., Visscher, K. & Brakenhoff, G. (1995a) Double-pulse fluorescence lifetime imaging in confocal micro-scopy. *J. Microsc.* **177**, 171–179.

Müller, M., Squier, J. & Brakenhoff, G.J. (1995b) Measurement of femtosecond pulses in the focal point of a high-numerical-aperture lens by two-photon absorption. *Opt. Lett.* **20**, 1038–1040.

Piston, D.W. & Webb, W.W. (1991) Three dimensional imaging of intracellular calcium activity using two-photon excitation of fluorescent indicator dye Indo-1. *Biophys. J.* **59**, 156.

Piston, D.W., Kirby, M.S., Cheng, H., Lederer, W.J. & Webb, W.W. (1994) Two-photon-excitation fluorescence imaging of three-dimensional calcium-ion activity. *Appl. Opt.* **33**, 662–669.

Piston, D.W., Masters, B.R. & Webb, W.W. (1995) Three-

dimensionally resolved NAD(P)H cellular metabolic redox imaging of the *in situ* cornea with two-photon excitation laser scanning microscopy. *J. Microsc.* **178**, 20–27.

Sheppard, C.J.R. & Gu, M. (1990) Image formation in two-photon fluorescence microscopy. *Optik*, **86**, 104–106. Erratum: (1992) *Optik*, **92**, 102.

Sheppard, C.J.R. & Gu, M. (1992) The significance of 3D transfer functions in confocal scanning microscopy. *J. Microsc.* **165**, 377–390.

Svoboda, K., Denk, W., W.H.K. & Tsuda, S. (1996) Two-photon-excitation scanning microscopy of living neurons with a saturable Bragg reflector mode-locked diode-pumped Cr:LiSrAlFl. *Opt. Lett.* **21**, 1411–1413.

Szmacinski, H., Gryczynski, I. & Lakowicz, J.R. (1996) Three-photon induced fluorescence of the calcium probe Indo-1. *Biophys. J.* **70**, 547–555.

Treacy, E.B. (1969) Optical pulse compression with diffraction gratings. *IEEE J. Quant. Electr.* **5**, 454–458.

Webb, W.W. (1990) Two photon excitation in laser scanning fluorescence microscopy. *Trans. R. Microsc. Soc.* (ed. by H. Y. Elder, pp. 445–450. Institute of Physics, Bristol.

Xu, C. & Webb, W.W. (1996) Measurement of two-photon excitation cross sections of molecular fluorophores with data from 690 to 1050 nm. *JOSA B*, **13**, 481–491.

Xu, C., Williams, R.M., Zipfel, W. & Webb, W.W. (1996) Multi-photon excitation cross-sections of molecular fluorophores. *Bioimaging*, **4**, 198–207.

Yu, W., So, T.C., French, T. & Gratton, E. (1996) Fluorescence generalized polarization of cell membranes: a two-photon scanning microscopy approach. *Biophys. J.* **70**, 626–636.